SPECIALIZED TRANSDUCTION BY BACTERIOPHAGE P22 IN *SALMONELLA TYPHIMURIUM*: GENETIC AND PHYSICAL STRUCTURE OF THE TRANSDUCING GENOMES AND THE PROPHAGE ATTACHMENT SITE

RUSSELL K. CHAN[1] AND DAVID BOTSTEIN[2]

Department of Biology, Massachusetts Institute of Technology, Cambridge, Massachusetts 02139

Manuscript received August 7, 1975

ABSTRACT

P22*pro-1* and P22*pro-3* are specialized transducing derivatives of phage P22 that carry the *proA* and *proB* genes of *Salmonella typhimurium*. These genes lie immediately adjacent to the prophage attachment site on the bacterial chromosome. By examining DNA heteroduplexes in the electron microscope, we found that DNA molecules from P22*pro-1* and P22*pro-3* each contain a substitution which adds length to the composite genome making the intracellular replicated genome too long to fit into a single phage particle. In this respect, and in many of their biological properties, the proline-transducing phages resemble P22Tc-10, another specialized transducing phage with an oversize, intracellular replicated genome which carries a tetracycline-resistance determinant from an R-factor.——Unlike P22Tc-10, however, P22*pro-1* and P22*pro-3* fail to integrate normally during lysogenizing infections, even when provided with all known integration functions. These results suggest that the proline substitutions have created a defect in the phage attachment site and suggest that the Campbell model for the formation of specialized transducing phages is applicable to phage P22 with the additional feature that oversize genomes can be produced and propagated.——A physical and genetic map of the P22 genome near the prophage attachment site was constructed which shows that the insertion from the R-factor in P22Tc-10 is not at the attachment site: it is therefore unlikely that P22Tc-10 was formed in an abnormal prophage excision event as envisioned in the Campbell model, but was instead the result of a direct translocation from the R-plasmid to P22.

TWO properties of the temperate phage P22 are important for understanding specialized transduction by this phage:

1) P22 integrates at a specific place on the *Salmonella typhimurium* chromosome (SMITH and LEVINE 1965, 1967; SMITH and STOCKER 1966; ITIKAWA and DEMEREC 1968). This suggests that, after induction, improper excision of the P22 prophage should produce specialized transducing phages carrying bacterial genes adjacent to the prophage attachment site on the bacterial chromosome (CAMPBELL 1962).

[1] Present address: Department of Genetics (SK-50), University of Washington, Seattle, Washington 98195.
[2] To whom reprint requests should be sent.

2) The chromosome of P22 is a linear duplex DNA molecule (27×10^6 daltons) which is circularly permuted and terminally repetitious (RHOADES, MACHATTIE and THOMAS 1968; TYE, CHAN and BOTSTEIN 1974; TYE, HUBERMAN and BOTSTEIN 1974). The perpetuation of circular permutation and terminal repetition during successive cycles of growth can be explained by the Streisinger model, which states that "headfuls" of DNA (somewhat longer than one genome in length) are encapsulated from a long DNA concatemer (STREISINGER, EMRICH and STAHL 1967). Drastic alterations in the genome size of a transducing phage resulting from the addition or substitution of host DNA do not prevent the transducing phage DNA from being encapsulated into P22 phage particles since the "headful" mechanism always packages a constant amount of DNA from the concatemer.

An insertion that makes the P22 genome too long to fit into a single phage head should result in the production of particles containing incomplete, but circularly permuted fragments of the intracellular replicated genome. This expectation was confirmed by genetic and physical studies on P22Tc-10, a P22 specialized transducing phage which contains an insertion of host DNA corresponding to 20% the length of a wild-type P22 genome (WATANABE *et al.* 1972; CHAN *et al.* 1972; TYE, CHAN and BOTSTEIN 1974; TYE, HUBERMAN and BOTSTEIN 1974).

Previous work on specialized transduction by P22 (SMITH-KEARY 1966; WING 1968; JESSOP 1972, 1976; HOPPE and ROTH 1974; KAYE, BARRAVECCHIO and ROTH 1974) had suggested that the Campbell model (CAMPBELL 1962) for the formation of lambda specialized transducing phages also applied to P22 since P22 was able to perform specialized transduction of bacterial genes adjacent to the prophage attachment site. However, the origin of P22Tc-10 appeared to be inconsistent with the Campbell model because the tetracycline resistance (tet^R) gene(s) carried by P22Tc-10 were derived from an *R factor* (WATANABE *et al.* 1972) which had no known attachment site for P22. Furthermore, ROTH and coworkers (HOPPE and ROTH 1974; KAYE, BARRAVECCHIO and ROTH 1974) used a procedure designed to yield transducing phages formed according to the Campbell model and found that none of the P22 specialized transducing phages they had isolated resembled P22Tc-10. Thus, we wondered if P22Tc-10 were a special case.

The electron microscopy of P22Tc-10 DNA seemed to confirm this notion: TYE, CHAN and BOTSTEIN (1974) found that the ends of the Tc-10 insertion contained an inverted repeat which was apparently identical to the inverted repeat SHARP, COHEN and DAVIDSON (1973) had found associated with the tet^R gene(s) on the *R* factor.

The present study concerns two specialized transducing derivatives of P22 isolated by JESSOP (1972, 1976), whose previous studies suggested that at least one of them might resemble P22Tc-10 in having a composite genome too large to fit into a single phage head. Both of these transducing phages (called P22*pro-1* and P22*pro-3*) contain genes (*proA* and *proB*) normally located immediately adjacent to the P22 prophage attachment site on the genetic map of *Salmonella*

typhimurium. The origin of these phages is consistent with the sort of abnormal excision of a prophage envisioned in the Campbell model.

Comparison of the proline-transducing phages with P22Tc-10 has enabled us to do the following:

1. Construct a physical and genetic map of phage P22 showing the relation of the prophage attachment site to the genes flanking it.
2. Infer that the *tet*^{R} insertion in P22Tc-10 was, in all probability, not the result of an abnormal prophage excision, but instead was the result of a direct transposition of the drug-resistance element from the *R*-factor to P22.
3. Demonstrate that the biological properties associated with oversize P22 genomes (i.e., genomes larger than a phage "headful") are independent of the origin of the extra DNA.

MATERIALS AND METHODS

Bacterial strains

The bacterial strains used are listed in Table 1. Prophage deletion strains are described in Figure 7 (CHAN and BOTSTEIN 1972).

UV-induced lysates of DB5425 and DB5426, which are lysogens (sent to us by A. JESSOP) of P22*pro-1* and P22*pro-3* respectively, were used to transduce DB141 to *pro*+ at a high multiplicity of infection (m.o.i.). All the *pro*+ transductants tested (about 10 for each lysate) gave the characteristic dark green color of unstable lysogens on green indicator plates (SMITH and LEVINE 1967). This was not surprising since DB141 contains the *proAB47* deletion (SMITH and LEVINE 1965) which removes *ataA*, the primary P22 prophage attachment site.

TABLE 1

*Bacterial strains**

Strain	Genotype	Synonym	Origin
DB21	*su*$^-$ prototroph	strain 18	BOTSTEIN (1968)
DB47	*su*$^-$ *rec*$^-$		BOTSTEIN and MATZ (1970)
DB53	*su*$^-$ *cysA1348hisC527*	TR248	J. ROTH
DB74	$su^+_{am}19$ *cysA1348hisC527*		BOTSTEIN and MATZ (1970)
DB98	*proA15*	*proA15*	MIYAKE and DEMEREC (1960)
DB124	*DB21(L)*		CHAN and BOTSTEIN (1972)
DB141*	[*gxu proB proA ataA*] ∇	*proAB47*	MIYAKE and DEMEREC (1960)
DB5000	*su*$^-$ *rec*+ (P22Tc-10)	Tc-10	WATANABE *et al.* (1972)
DB5055	[*leuD798ara*] ∇ *fol-101 his1099 trpA50*	PM452	P. MARGOLIN
DB5202	DB21 (P22c_2-*ts30*m_3*sieA1sieB1*)		This paper
DB5204	DB21 (P22Tc-10 c_2-*ts30sieA1sieB1*)		CHAN *et al.* (1972)
DB5425*	*proAB47* (P22*pro-1*)	Ih(39)	JESSOP (1972)
DB5426	*proB436* (P22*pro-3*)	C_1h(5)	JESSOP (1972)
DB5524	DB53 (P22Tc-10 c_2-*ts30sieA1sieB1*)		This paper
DB5732*	DB141 (P22*pro-1*)		This paper
DB5733*	DB141 (P22*pro-3*)		This paper

* All strains are derivatives of *Salmonella typhimurium* LT-2, except for DB141, DB5425, DB5732 and DB5733, which are derivatives of *Salmonella typhimurium* LT-7.

When these *pro*+ transductants were purified three times on minimal plates (i.e., selecting for *pro*+), the resulting colonies appeared to be stably integrated by the criterion of colony color on green indicator plates. A stable lysogen derived from each lysogen was saved; these lysogens (DB5732 and DB5733) are the source of all the P22*pro-1* and P22*pro-3* lysates used in this paper.

Phage strains

The following P22 strains, derived from the wild-type strain of LEVINE (1957) were used: *c*+, the wild-type phage, c_2-5, a clear-plaque mutant which does not lysogenize (LEVINE and CURTISS 1961); *int3*, an integration-deficient mutant (SMITH and LEVINE 1967); *mnt1*, a mutant which is unable to maintain lysogeny (GOUGH 1968); m_3*sieA1sieB1*c_2-*ts30* [*sieA1* and *sieB1* are mutations which remove the prophage superinfection exclusion system (SUSSKIND, WRIGHT and BOTSTEIN 1971); c_2-*ts30* makes the prophage heat-inducible]. The plaque morphology markers m_3 and h_{21} have been described previously (LEVINE and CURTISS 1961).

P22*bp1* tet^R [*att int*]▽, which contains a deletion which removes the phage attachment site and at least part of the *int* gene, was isolated as a non-defective, large plaque-forming revertant from a high-frequency-transducing lysate of defective P22Tc-10 particles (CHAN *et al.* 1972; TYE, CHAN and BOTSTEIN 1974).

P22*cp1* [*att*]▽ was isolated as a large plaque-forming revertant from a P22*pro-1* lysate.

Phage L (BEZDEK and AMATI 1968) is a temperate Salmonella phage heteroimmune to P22 but very closely related to it (BOTSTEIN, CHAN and WADDELL 1972).

Media

LB broth, lambda agar, soft top agar, minimal top agar, dilution fluid, and buffered saline are described in EBEL-TSIPIS and BOTSTEIN (1971). Minimal medium containing amino acids (M9CAA) is described by SMITH and LEVINE (1964). Minimal agar is M9 medium (no amino acids) with 1.5% agar (w/v). Green indicator agar is described by CHAN *et al.* (1972).

Complementation test for lysogeny

The complementation test is essentially that described by SMITH and LEVINE (1967). Cells (either DB21, DB74, or DB98) were infected with each of two phages to be tested. The multiplicity of infection of c_2-5, *int3*, *mnt*, *bp1*, and *cp1* was 10 PFU/ml; the multiplicity of infection of P22*pro-1* was 60 particles/cell and of P22*pro-3* was 10 particles/cell where the particle titer was estimated by determining the absorbance at 260 nm (see Table 2). The infected cells were spread on green indicator plates and incubated at 37° overnight.

TABLE 2

*The relative titer of defective particles in a P22Tc-10, P22*pro-1, *and P22*pro-3 *lysate**

Lysate	Particle titer estimated by A_{260}†	Plaque formation on a P22 prophage deletion strain (DB147)‡	Plaque formation on a sensitive, nonlysogenic strain (DB21)§
P22Tc-10¶	1.0	.06	5.0×10^{-5}
P22*pro-1*	1.0	.02	1.0×10^{-6}
P22*pro-3*	1.0	.55	1.3×10^{-2}

* For each lysate, the titers are normalized to the titer estimated at A_{260}.

† The particle titer was estimated by measuring the absorbance at 260 nm (A_{260}) of CsCl-purified particles and dividing by the optical cross section of wild-type P22 particles (1.8×10^{-12} A_{260}/PFU at 1 cm path length (SMITH 1968; CHAN, unpublished).

‡ DB147 is a *pro*⁻ P22 prophage deletion strain (CHAN *et al.* 1972).

§ For P22Tc-10 and P22*pro-1*, only large plaques were counted because only large plaques plate linearly. Since all plaques in a P22*pro-3* lysate plate linearly, all P22*pro-3* plaques were counted.

¶ The values for P22Tc-10 are taken from CHAN *et al.* (1972).

Unstably lysogenized colonies appear dark green or blue on green indicator plates, whereas stably-lysogenized or uninfected, sensitive colonies appear white or yellow. Therefore, in each case, about 30 white colonies were tested because all the other colonies on the plate were green. Two phages were said to complement if immune, stably-lysogenized colonies were found. The presumptive lysogens were further tested for the ability to produce phage upon UV-induction.

The isolation of gxu-pro⁻ *P22 prophage deletions*

We developed a simple, positive selection on solid medium for P22 prophage deletions by simultaneously selecting for 8-azaguanine-resistance ($8AG^R$) and for survival at the nonpermissive temperature of a temperature-inducible (c_2-*ts*) lysogen. The rationale for this procedure is based on the observation by GOTS, BENSON and SHUMAS (1972) that a gene (called *gxu*) required for *g*uanine and *x*anthine *u*tilization maps to the left of the *proB* and *proA* (proline biosynthesis genes) and of *ataA* (the P22 prophage attachment site) on the Salmonella chromosome (see FIGURE 7); loss of the *gxu* function results in resistance to 8-azaguanine.

A stock solution of 8-azaguanine (Calbiochem) at 10 mg/ml was made in 0.2 M NaOH.

Aliquots of independent overnight cultures of a P22c_2-*ts* lysogen were spread on minimal plates containing 8-azaguanine (100 μg/ml) and proline (20 μg/ml), warmed to 40°, and incubated for 2 days at 40°.

Two colony sizes are seen among the survivors on the plate: the small colonies occur at a frequency of 10^{-6}, whereas large colonies occur at a frequency of 6×10^{-8}. The large colonies, which we presume are truly resistant to 8-azaguanine ($8AG^R$) were purified by single-colony isolation at 40° on minimal plates supplemented with 8AG and proline and tested for *pro*⁻ and immunity. Colonies which were *pro*⁻ and nonimmune were then tested for the presence of phage genes as described by CHAN and BOTSTEIN (1972).

Preparation of phage stocks

Lysates of P22*pro-1*, P22*pro3*, and P22Tc-10 were prepared by UV-induction of the appropriate lysogens in M9CAA as described by CHAN *et al.* (1972), except that purified base-plate parts (ISRAEL, ANDERSON and LEVINE 1967; ISRAEL 1967) were not added to lysates of P22*pro-1* and P22*pro-3* because the particles in these lysates are not base-plate-deficient.

P22m_3c_2-*5*h_{21} was prepared by infecting DB21 (about 3×10^7 cells/ml) in LB at an m.o.i. of 0.01 and shaking at 30° for 3½ hours.

P22*bp1* was grown on DB21 by the plate stock method (ADAMS 1959).

Preparation of phage DNA

Phage DNA was prepared from purified phage particles as described by TYE, CHAN and BOTSTEIN (1974).

Electron microscopy of DNA heteroduplexes

The method of DAVIS, SIMON and DAVIDSON (1971) as modified by TYE, CHAN and BOTSTEIN (1974) was used.

RESULTS

*P22*pro-1 *and P22*pro-3 *transducing genomes*

Previous work (JESSOP 1972, 1976) had suggested that P22*pro-1*, like P22Tc-10, might have an insertion of host DNA which adds length to the composite genome making the intracellular, replicated genome too long to fit into a single phage head. To look for that insertion, we prepared heteroduplexes between P22*pro-1* DNA and P22Tc-10 DNA. In such preparations, heteroduplex molecules can be distinguished from homoduplex molecules by the presence of the lariat-shaped Tc-10 insertion (TYE, CHAN and BOTSTEIN 1974); furthermore, the location of the proline genes relative to the Tc-10 insertion is revealed by the structure of a *pro-1*/Tc-10 heteroduplex.

The pro-1/*Tc-10 heteroduplex*: The heteroduplex between P22*pro-1* DNA and P22Tc-10 DNA (Figure 1a) is circular because the two strands which make up the duplex are circularly permuted with respect to each other. The characteristic Tc-10 stem and loop structure as well as a large substitution in the heteroduplex due to *pro-1* are traced in Figure 2a and interpreted in Figure 3a.

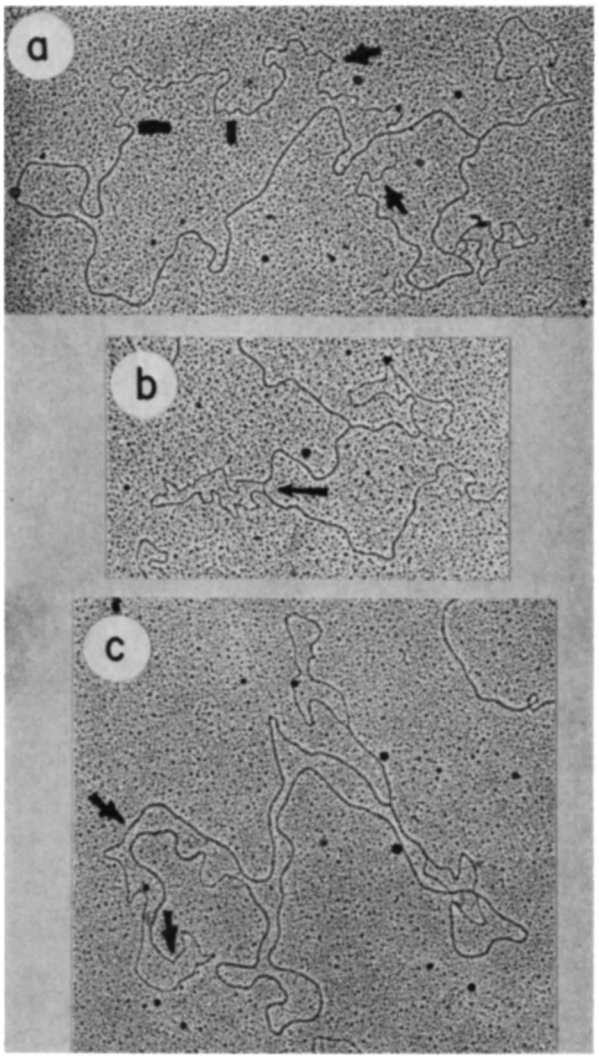

FIGURE 1.—DNA heteroduplexes between P22Tc-10 and the proline transducing phages. (a) P22Tc-10/P22*pro-1*. The limits of one single-stranded region are marked by the arrows; the limits of the second single-stranded region are marked by the bars. (b) A section of a P22Tc-10/P22*pro-1* heteroduplex which shows the structure of the *pro-1* substitution very clearly. The arrow points to the small deletion segment at the base of the *pro-1* substitution. (c) P22Tc-10/P22*pro-3*. The limits of the single-stranded region are marked by the arrows.

Tracings of the regions of nonhomology in these heteroduplexes are shown in Figure 2.

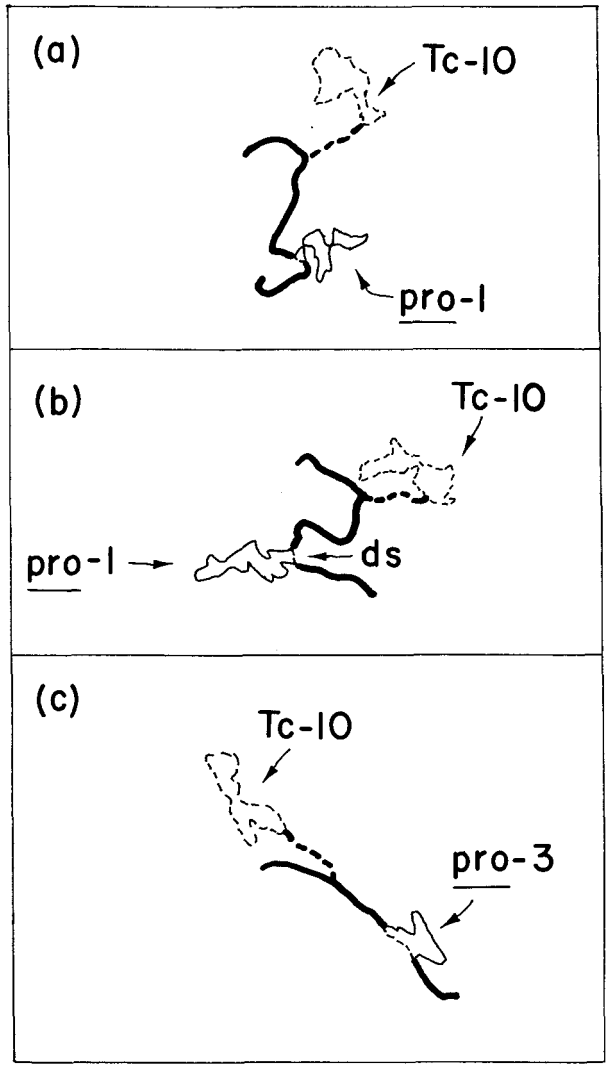

FIGURE 2.—Tracings of nonhomologous regions of the DNA heteroduplexes in Figure 1.
(a) & (b). P22Tc-10/P22*pro-1*
(c). P22Tc-10/P22*pro-3*
The double-stranded regions are represented by the thick solid line. The double-stranded stem of the Tc-10 insertion is represented by the thick dashed line. The single strand belonging to P22Tc-10 is represented by the thin dashed line. The single strand belonging to the proline phage is represented by the thin line. In panel (b), the symbol (ds) refers to the deletion segment at the base of the *pro-1* substitution.

If the *pro-1* substitution resulted in a net loss of DNA from the phage genome, the mature *pro-1* chromosome would be expected to have more terminal repetition than wild type since P22 is packaged by a "headful" mechanism (STREISINGER, EMRICH and STAHL 1967; TYE, CHAN and BOTSTEIN 1974; TYE, HUBER-

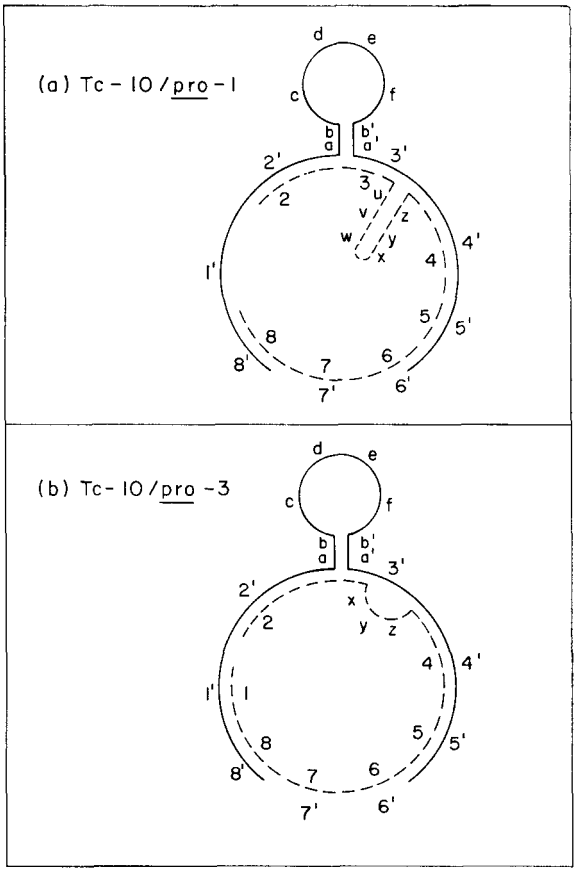

FIGURE 3.—A schematic diagram showing our interpretation of the DNA heteroduplexes between P22Tc-10 and the proline phages. The solid line represents the Tc-10 DNA strand; the dashed line represents the proline phage DNA strand.

MAN and BOTSTEIN 1974). However, the *pro-1* chromosome appears to have no terminal repetition at all, since no single-stranded branches are found on the circular *pro-1*/Tc-10 heteroduplex. Thus, we conclude that the P22*pro-1* substitution, like the Tc-10 insertion, results in a net increase in the length of the phage genome.

There are two single-stranded regions in the circumference of the circular heteroduplex (marked by the arrows and bars in Figure 1a; diagrammed in Figure 3a); one single-stranded region must correspond to the ends of the incomplete P22Tc-10 DNA strand and the other must correspond to the ends of the incomplete P22*pro-1* DNA strand (see Figure 3a).

Eleven circular heteroduplexes were photographed and measured. The *pro-1* substitution, which is located near the site of the Tc-10 insertion, is composed of a 13% insertion and a 0.4% deletion.

We cannot rule out the possibility that the small deletion segment at the base of the *pro-1* substitution (see Figures 1b and 2b) is an artifact of the spreading conditions since such an artificial denaturation is sometimes seen at the base of the deletion/insertion loop in heteroduplexes of the simple deletion mutant *λb2* (M. M. GOTTESMAN, personal communication; R. W. DAVIS, personal communication). Nevertheless, we believe that the tiny deletion segment is real since we have seen it in photographs of 40 molecules and in many more molecules directly in the electron microscope. In any case, either interpretation of the structure of *pro-1* is compatible with our explanation for the origin of P22*pro-1*.

The pro-1/*wild-type heteroduplex*: Heteroduplexes were prepared between P22 wild-type DNA and P22*pro-1* DNA. The structure and dimensions of the *pro-1* substitution in these circular heteroduplexes were identical to the structure and dimensions of the *pro-1* substitution in the *pro-1*/Tc-10 circular heteroduplexes described above.

The pro-3/*Tc-10 heteroduplex*: The DNA heteroduplex experiments used to determine the structure of P22*pro-1* DNA were repeated with P22*pro-3* DNA. Figure 1c shows a typical *pro-3*/Tc-10 circular heteroduplex with the Tc-10 insertion and a substitution due to *pro-3*. Like the *pro-1*/Tc-10 circular heteroduplex, the *pro-3*/Tc-10 circular heteroduplex has no single-stranded branches. This suggests that the *pro-3* substitution, like the *pro-1* substitution and the Tc-10 insertion, results in a net increase in the length of the phage genome relative to wild type such that the "headful" packaging mechanism produces mature DNA molecules with no terminal repetition (STREISINGER, EMRICH and STAHL 1967; TYE, CHAN and BOTSTEIN 1974).

Knowing that the genome of P22*pro-3* is longer than wild type, we can assign the long strand in the substitution loop to P22*pro-3* (see Figures 1c, 2c and 3b).

Eleven circular heteroduplexes were measured. The *pro-3* substitution, like the *pro-1* substitution, is located near the site of the Tc-10 insertion, but consists of a 6% insertion and a 3% deletion.

The pro-3/*wild-type heteroduplex*: Heteroduplexes were prepared between P22 wild-type DNA and P22*pro-3* DNA. The structure and dimensions of the *pro-3* substitution in these circular heteroduplexes were identical to the structure and dimensions of the *pro-3* substitution in the *pro-3*/Tc-10 circular heteroduplexes described above.

The pro-1/pro-1 *and* pro-3/pro-3 *DNA homoduplexes*: The preceding experiments showed that the P22*pro-1* genome is 13% longer than a wild-type genome and that the P22*pro-3* genome is 3% longer than a wild-type genome, whereas a normal headful of P22 DNA is just 2% longer than the length of the wild-type genome (this follows from the fact that the wild-type terminal repetition is about 2% (RHOADES, MACHATTIE and THOMAS 1968; TYE, CHAN and BOTSTEIN 1974)). Therefore, the P22*pro-1* and P22*pro-3* genomes are too long to fit into a single phage head; incomplete, but circularly permuted DNA molecules will be encapsulated by the headful packaging mechanism. These P22*pro-1* and P22*pro-3* DNA molecules, like P22Tc-10 molecules (TYE, CHAN and BOTSTEIN 1974), are

able to form circular homoduplexes lacking terminally repetitious ends (data not shown; CHAN 1974).

*P22*pro-1 *and P22Tc-10 have similar plaque-forming properties*

Now we describe the properties of P22*pro-1* that originally led us to believe that P22*pro-1*, like P22Tc-10, contained an insertion of host DNA which added length to the composite genome making it too long to fit into a single phage head. These results confirm similar observations by JESSOP (1972, 1976).

When a P22*pro-1* lysate is plated on a sensitive, *pro*$^-$ indicator strain, small plaques and large plaques are seen; the turbid centers of small plaques contain *pro*$^+$ transductants, whereas the turbid centers of large plaques do not. Plaque formation by small plaques (Figure 4a) is multiplicity-dependent. The frequency of large plaques in a P22*pro-1* lysate is so low (never more than 5% of total plaques) that the high background of small plaques makes it difficult to count statistically significant numbers of large plaques. To reduce the high background of small plaques, we plated the P22*pro-1* lysate on a *rec*$^-$ indicator strain (see CHAN 1974 for details). The results plotted in Figure 4b indicate that the large plaques from a P22 *pro-1* lysate increase linearly.

JESSOP (1972) showed that there were many more particles in a P22*pro-1* lysate, as estimated from electron microscope counts or from assay of *pro*$^+$ transductants, than there were plaque-forming units, as estimated by plating on sensitive cells. These defective particles can also be assayed by plating on P22 prophage deletion strains or on a lysogen of the heteroimmune phage L. Further-

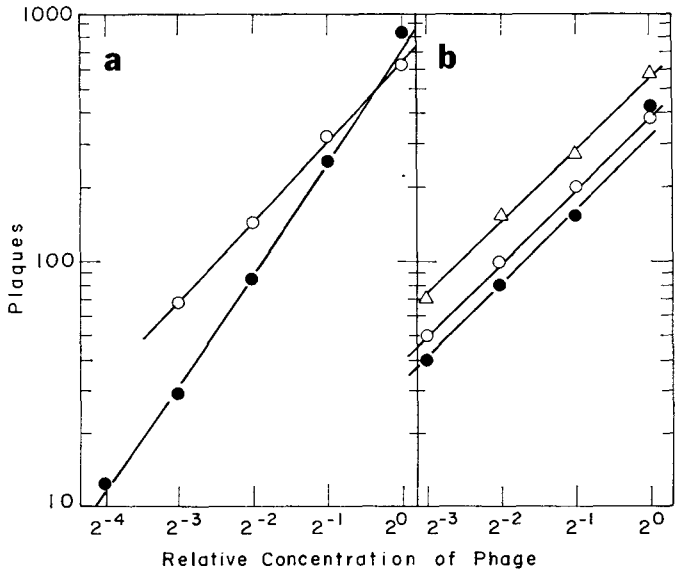

FIGURE 4.—Concentration dependence of the plaque assay. (a) ● P22*pro-1* small plaques on DB21; ○, P22*pro-3* on DB21. DB21 is a nonlysogen. (b) ○, P22*pro-1* on DB124; △, P22*pro-3* on DB124; ●, P22*pro-1* large plaques on DB47. DB124 is lysogenic for the heteroimmune phage L; DB47 is *rec*$^-$. For each case, the data from an arbitrary set of serial dilutions is shown.

more, the plaques from a P22*pro-1* lysate which appear on a heteroimmune lysogen (DB124) increase as a linear function of the concentration (Figure 4b) in contrast to the small plaques from a P22*pro-1* lysate that do not increase linearly (Figure 4a) on a nonlysogenic indicator (DB21).

The number of particles in our P22*pro-1* lysate can be estimated by measuring the absorbance at 260 nm (SMITH 1968; see also CHAN *et al.* 1972). Using this measure, we find that there are 10^6-fold more particles in a P22*pro-1* lysate than there are large-plaque-forming phage (Table 2). No particular essential region of the genome must be missing from all of these defective particles since overlapping prophage deletions each can support growth of a substantial number of defective particles (data not shown; CHAN 1974).

These plaque-forming properties of a P22*pro-1* lysate are consistent with the physical structure of the P22*pro-1* genome. The *pro-1* substitution makes the phage genome too long to fit into a single phage head; therefore, the headful packaging mechanism encapsulates incomplete but circularly permuted fragments of the intracellular replicated genome. The particles containing these incomplete chromosomes are defective upon single infection, but can cooperate with each other to grow in a multiple infection, thereby producing P22*pro-1* small plaques which show a multiplicity-dependence. These defective particles can also be rescued by recombination with the phage DNA present in P22 prophage deletion strains or in lysogens of the heteroimmune phage L. The large plaques, which appear as a linear function of the concentration, arise from revertant phages which have lost the insertion of proline genes; the genome of these revertants has become short enough to fit into a phage particle again.

*P22*pro-3 *does not have the same plaque-forming properties as P22*pro-1 *and P22Tc-10*

Unlike a P22*pro-1* lysate, a P22*pro-3* lysate makes small plaques that increase linearly (Figure 4a; see also JESSOP 1976); the turbid centers of these plaques contain *pro*$^+$ transductants. Thus, P22*pro-3* might at first appear to be a nondefective P22 specialized transducing phage. However, the titer of a P22*pro-3* lysate can be increased up to 50-fold by plating on certain P22 prophage deletion strains (CHAN 1974; see also JESSOP 1976). These additional particles which are responsible for forming plaques on prophage deletion strains can also be detected physically by measuring the absorbance at 260 nm of CsCl-purified particles (Table 2). Thus, about 50% of the particles in a P22*pro-3* lysate can form plaques on certain prophage deletion strains, whereas only 1% can form plaques on a sensitive, non-lysogenic strain.

Physical and genetic mapping of the Tc-10 insertion and of the pro-1 *and* pro-3 *substitutions*

The *pro-1*/Tc-10 and *pro-3*/Tc-10 DNA heteroduplexes above showed that both proline substitutions were located close to the site of the Tc-10 insertion. To determine whether both proline substitutions were on the same side of the Tc-10 insertion, the proline substitutions were mapped with respect to another marker.

For this purpose, we chose the *bp1* deletion, a derivative of P22Tc-10, which removes the phage attachment site and the *int* gene but retains part of the tet^R insertion (CHAN *et al.* 1972; TYE, CHAN and BOTSTEIN 1974).

The pro-1/bp1 *and* pro-3/bp1 *heteroduplex*: Heteroduplexes between P22*pro-1* DNA and P22*bp1* DNA were prepared and examined in the electron microscope. All the circular heteroduplexes observed had only one region of nonhomology (see Figures 5a and 6a), indicating that the site of the *pro-1* substitution overlaps the region deleted by *bp1*.

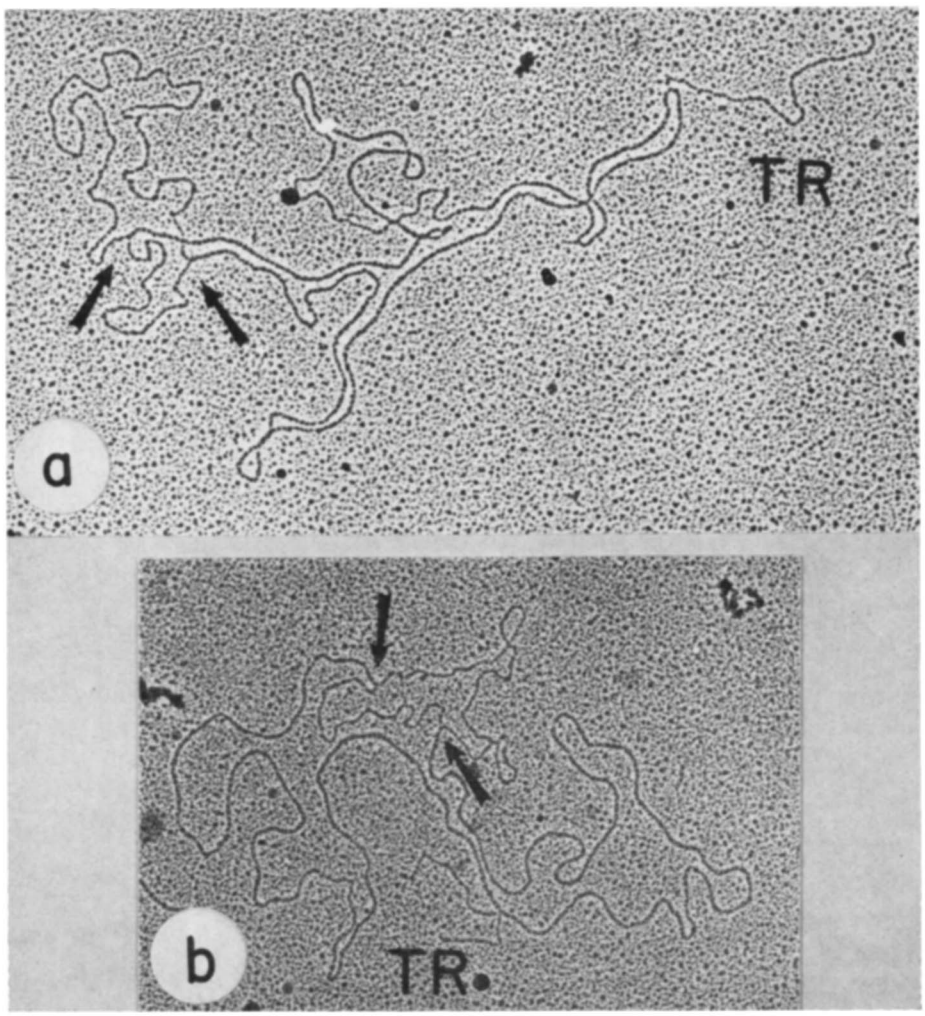

FIGURE 5.—DNA heteroduplexes between P22*bp1tet*^{R} [*att int*]▽ and the proline phages.
(a) P22*bp1*/P22*pro-1*
(b) P22*bp1*/P22*pro-3*
The nonhomologous region in each heteroduplex is indicated by the arrows and is also traced in Figure 6. The terminal repetition (TR) is also labeled.

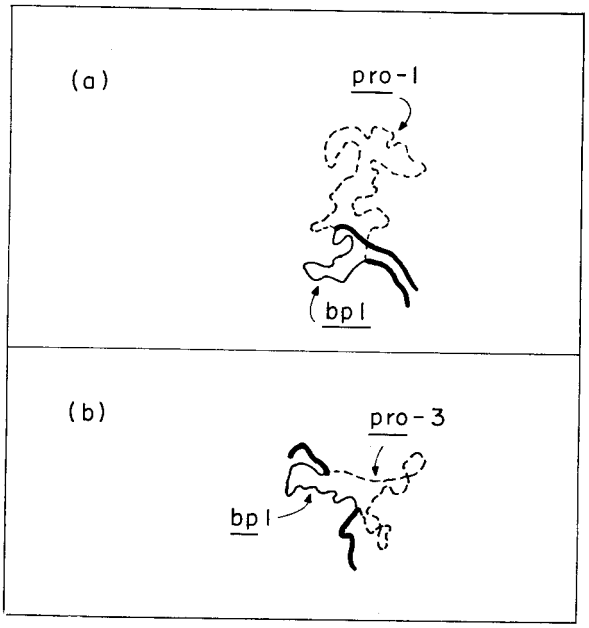

FIGURE 6.—Tracings of the nonhomologous regions of the DNA heteroduplexes shown in Figure 5.

(a) P22*bp1*/P22*pro-1*

(b) P22*bp1*/P22*pro-3*

The double-stranded regions are represented by the thick line. The single strand belonging to P22*bp1* is represented by the thin line. The single strand belonging to the proline phage is represented by the thin dashed line. The logic of the strand assignments is presented in the DISCUSSION and Figure 9.

If the *pro-3* substitution is on the same side of the Tc-10 insertion as the *pro-1* substitution, the *pro-3* substitution should also overlap the region deleted by the *bp1* deletion. Heteroduplexes between P22*pro-3* and P22*bp1* DNA were prepared and examined in the electron microscope. The circular *pro-3*/*bp1* DNA heteroduplex has only one region of nonhomology (Figure 5b, 6b), indicating that the *pro-3* substitution, like the *pro-1* substitution, overlaps the region deleted by P22*bp1tet*^{R} [*att int*]∇.

Genetic mapping of the Tc-10 insertion: The heteroduplex mapping described above showed that both proline substitutions are close to the site of the Tc-10 insertion and that both substitutions are on the same side of the Tc-10 insertion. In this section, we describe the genetic mapping of the Tc-10 insertion that will enable us to determine the genetic location of the proline substitutions.

Previously, TYE, CHAN and BOTSTEIN (1974) had concluded that the Tc-10 insertion must be near the *int* gene and the phage attachment site because a single deletion such as the *bp1* deletion simultaneously removed part of *int* and *att* as well as part of the Tc-10 insertion. This conclusion is confirmed by our deletion mapping of the P22Tc-10 prophage. Figure 7 shows that every prophage deletion

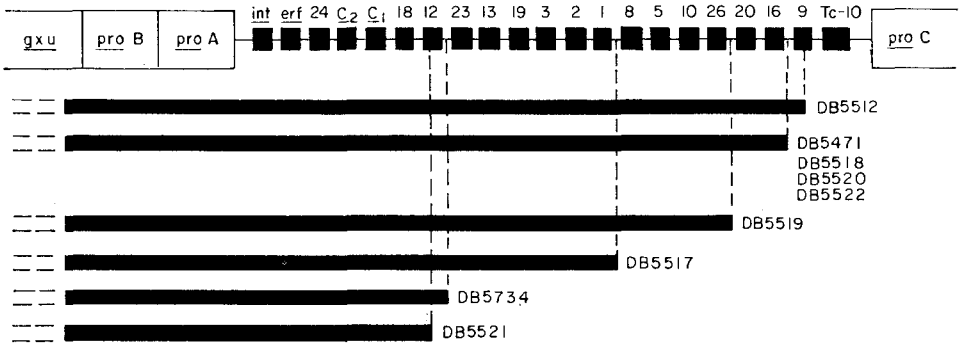

FIGURE 7.—Deletion mapping of the Tc-10 insertion. The bars represent the deleted material in these *gxu⁻pro⁻* P22 prophage deletion strains which were isolated from a lysogen of P22Tc-10 c_2-*ts30* by simultaneous selection for resistance to 8-azaguanine and survival at high temperature as described in the MATERIALS AND METHODS.

strain isolated (including DB5512 whose deletion falls within gene *9*, the rightmost essential gene) was *tet*^{R}. Thus, the *tet*^{R} gene(s) are located to the right of gene *9* on the *proC* side of the P22 prophage. Furthermore, all the genes required to define the Tc-10 genotype are located there, too, because the P22Tc-10 phage can efficiently be reconstructed by recombination between P22 wild type and the *tet*^{R} gene(s) which remain in the prophage deletion strain DB5512 (Figure 7).

Since the vegetative genetic map of P22 is circular (GOUGH and LEVINE 1968), the gene order around the phage attachment site must be *9*–Tc-10–*att*–*int*. The proline/Tc-10 heteroduplexes showed that the proline substitutions were close to the site of the Tc-10 insertion but did not specify on which side. We can place the proline substitutions on the *att* side of theTc-10 insertion because the proline/*bp1* heteroduplexes show that the proline substitutions overlap the region deleted by the *bp1* deletion which removes *int*, *att*, and part of the Tc-10 insertion (CHAN *et al.* 1972; TYE, CHAN and BOTSTEIN 1974). Thus, we deduce the following map order: *9*–Tc-10–(*pro-1*, *pro-3*, *att*)–*int*.

*The P22*pro-1 *and P22*pro-3 *substitutions cause a defect in prophage attachment*

The preceding results suggest that the attachment site (*att*) of P22 is near the site of the proline substitutions in both P22*pro-1* and P22*pro-3*. In the case of coliphage λ, such substitutions cause a non-complementable (i.e., *cis*-dominant) defect in prophage integration. If the proline transducing phages are both actually the result of an aberrant excision of a P22 prophage, then one might expect a similar defect in these phages.

Although the prophage attachment site on the Salmonella chromosome is intact in strain DB98 (a proline-requiring strain which carries the point mutation *proA15*), *pro*$^+$ transductants of DB98 made from a P22*pro-1* lysate give an "unstable" response when streaked on green indicator plates (SMITH and LEVINE 1967). If sensitive cells superinfected with P22*pro-1* at a high multiplicity of infection are plated directly on green indicator plates (i.e., no selection for *pro*$^+$), the colonies still appear unstable; JESSOP (1976) has made similar observations.

Any mutation that prevents P22 from integrating will give this "unstable" response on green indicator plates (SMITH and LEVINE 1967; GOUGH 1968). The defect can be in the phage (e.g., P22*mnt*$^-$ or P22*int*$^-$) or in the bacterium (e.g., a Salmonella strain deleted for the prophage attachment site on the bacterial chromosome).

In order to characterize the defect leading to this unstable response, a P22*pro-1* lysate was tested for complementation with P22c_2^- (c_2 is the gene for the *immC* repressor; LEVINE 1957, 1972; CHAN and BOTSTEIN 1972), P22*mnt*$^-$ (*mnt* is the gene for a second (*immI*) repressor, which is required for the *maint*enance of lysogeny; GOUGH 1968; LEVINE 1972; CHAN and BOTSTEIN 1972), P22*int*$^-$ (the *int* gene product is required for integration of the phage into the chromosome; SMITH and LEVINE 1967), and P22*bp1tet*^{R} [*att int*]∇ (P22*bp1* has a deletion that removes the phage attachment site and the *int* gene; CHAN *et al.* 1972; TYE, CHAN and BOTSTEIN 1974). As shown in Table 3, P22*pro-1* can complement P22c_2^-, P22*mnt*$^-$, and P22*int*$^-$ for lysogeny, but fails to complement P22*bp1* for lysogeny. We conclude that P22*pro-1* must have an altered or defective phage attachment site, but that *mnt*, *int*, and c_2 genes are intact in P22*pro-1*.

An alteration in the phage attachment site would be expected to affect the establishment of lysogeny but not the stability of lysogens after they have been formed. This expectation is confirmed by the observation that the rare lysogens (i.e., *pro*$^+$ transductants) which are formed after infection by P22*pro-1* are as stable as wild-type P22 lysogens. They give the stable wild-type response on green indicator agar.

In a previous section, we concluded that the *pro-1* substitution is located near the phage attachment site because it overlaps the *bp1* deletion, which removes the phage attachment site and at least part of the *int* gene. Thus, it seems reasonable to assume that the defect in the attachment site of P22*pro-1* is caused by the *pro-1* substitution.

Like P22*pro-1*, P22*pro-3* fails to integrate (JESSOP 1976), complements P22c_2^-, P22*mnt*$^-$, and P22*int*$^-$ for lysogeny, but fails to complement P22*bp1* (Table 3). Therefore, P22*pro-3* also appears to have an altered or defective phage attachment site, while retaining the c_2, *mnt*, and *int* genes intact.

TABLE 3

Complementation for lysogeny*

	Alone	P22c_2-5	P22*mnt1*	P22*int3*	P22*bp1*†
Alone		0	0	0	0
P22*pro-1*	0	+	+	+	0
P22*pro-3*	0	+	+	+	0
P22*cp1*	0	+	+	+	0

* The complementation was performed as described in MATERIALS AND METHODS. 0 = no stable lysogens found among the 100–200 colonies scored. + = at least one stable lysogen found. P22*cp1* is a large-plaque-forming phage derived from P22*pro-1*.

† P22*bp1* has a deletion that covers the phage attachment site and the *int* gene.

A large plaque-forming revertant (designated P22*cp1*) isolated from a P22 *pro-1* lysate no longer transduces *pro*$^+$, but resembles the P22*pro-1* lysate in its ability to complement P22c_2^-, P22*mnt*$^-$, and P22*int*$^-$, but not P22*bp1* for lysogeny (Table 3). We conclude that P22*cp1*, like P22*pro-1*, must have an altered or defective phage attachment site and an intact *mnt*, *int*, and c_2 gene. P22*cp1* is therefore a useful tester phage since it is the first plaque-forming P22 phage that is *att*$^-$*int*$^+$, and thus resembles *λb2* (KELLENBERGER, ZICHICHI and WEIGLE 1961).

DISCUSSION

In previous work (WATANABE *et al.* 1972; CHAN *et al.* 1972; TYE, CHAN and BOTSTEIN 1974) on specialized transduction with P22Tc-10, we described how a phage with a headful mechanism for the encapsulation of DNA (STREISINGER, EMRICH and STAHL 1967) could accommodate a large insertion of host DNA that made the composite genome too long to fit into a single phage particle. In particular, we showed that P22Tc-10 could package incomplete, but circularly permuted fragments of its intracellular replicated genome. In order to show that the major properties of P22Tc-10 were not restricted to P22 specialized transducing phages carrying insertions derived from *R* factors, we began the study of P22*pro-1* and P22*pro-3* reported here.

Our results can be briefly summarized: P22*pro-1* and P22*pro-3* each contain a substitution of host DNA that adds length to the composite genome, making it too long to fit into a single phage particle. Nevertheless, incomplete and circularly permuted fragments of these intracellular replicated genomes are encapsulated by the headful packaging mechanism. The plaque-forming properties of P22*pro-1* are similar to those of P22Tc-10. Using physical and genetic methods, we have determined the following map order in the vicinity of the phage attachment site: *9*–Tc-10–(*pro-1*, *pro-3*, *att*)–*int*. Thus, the *pro-1* and *pro-3* substitutions are located close to, but not at, the same site as the Tc-10 insertion. Unlike P22Tc-10, P22*pro-1* and P22*pro-3* behave as though they are defective in the phage attachment site.

Physical mapping of the P22 genome

Summary of measurements: Our measurements of the *pro-1* and *pro-3* DNA heteroduplexes are summarized in Figure 8. Within the limits of error, the dimensions of each proline substitution are identical whether proline phage DNA was reannealed with Tc-10 DNA (Figures 8a, b) or with wild-type phage DNA (Figures 8c, d). Likewise, the dimensions of the Tc-10 insertion are identical in our two preparations (Figures 8a, b) and are identical to those reported by TYE, CHAN and BOTSTEIN (1974).

In the heteroduplexes between P22*bp1* DNA and proline phage DNA, we assigned the long strand in the region of nonhomology to the proline-transducing phage (Figures 8e, f) because the circular *bp1/pro* DNA heteroduplexes had only one single-stranded branch (see Figures 5a, b and 9a, b) which must correspond

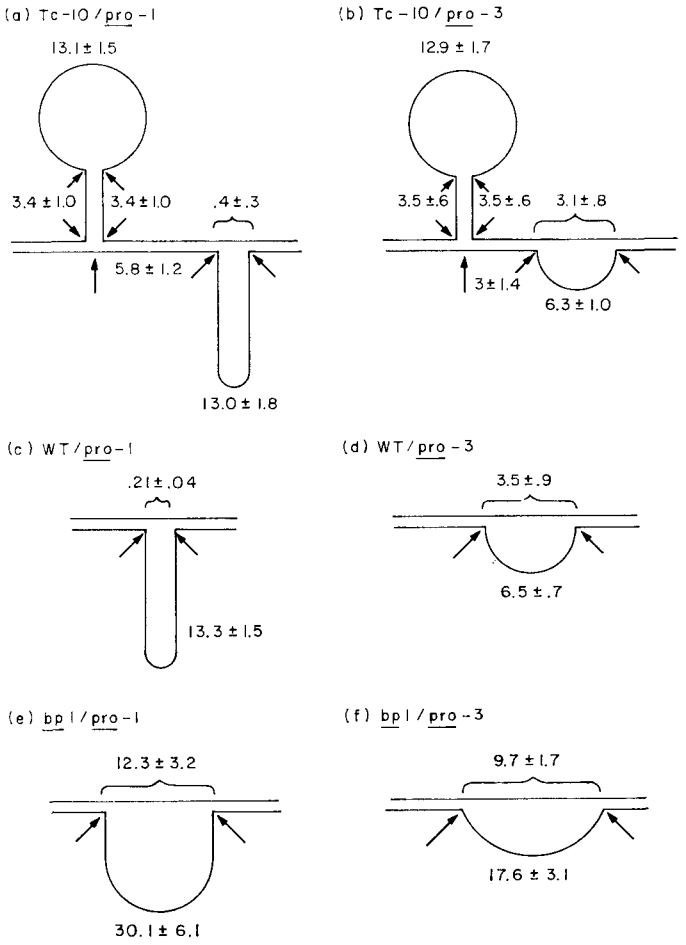

FIGURE 8.—A summary of measurements of the regions of nonhomology in circular DNA heteroduplexes involving P22*pro-1* and P22*pro-3*. In each case the lower DNA strand belongs to the proline-transducing phage. The measurements pertain to the segments marked by the arrows. The segment lengths (given as the mean ± standard deviation) are expressed as a percent of the heteroduplex circumference. The circumference of the Tc-10/*pro-1*, Tc-10/*pro-3*, WT/*pro-1*, WT/*pro-3* heteroduplexes is equivalent to the length of a wild-type genome. The circumference of the *bp1/pro-1* and *bp1/pro-3* heteroduplexes is equivalent to the length of the *bp1* genome which is 5% shorter than a wild-type genome (TYE, CHAN and BOTSTEIN 1974). The number of molecules measured for each heteroduplex is as follows: (a) 11, (b) 11, (c) 7, (d) 7, (e) 7, (f) 10.

to the terminally repetitious end of the *bp1* chromosome (TYE, CHAN and BOTSTEIN 1974). Since each mature P22 DNA molecule must be the same length (i.e., one headful), the long strand in the nonhomology loop must belong to the proline phage. The length of each strand in the nonhomology region of the *pro/bp1* heteroduplexes is also consistent with what we already know about the size of the proline substitutions and the size of the *bp1* insertion-deletion. TYE, CHAN and BOTSTEIN (1974) showed that the length of the wild-type strand in

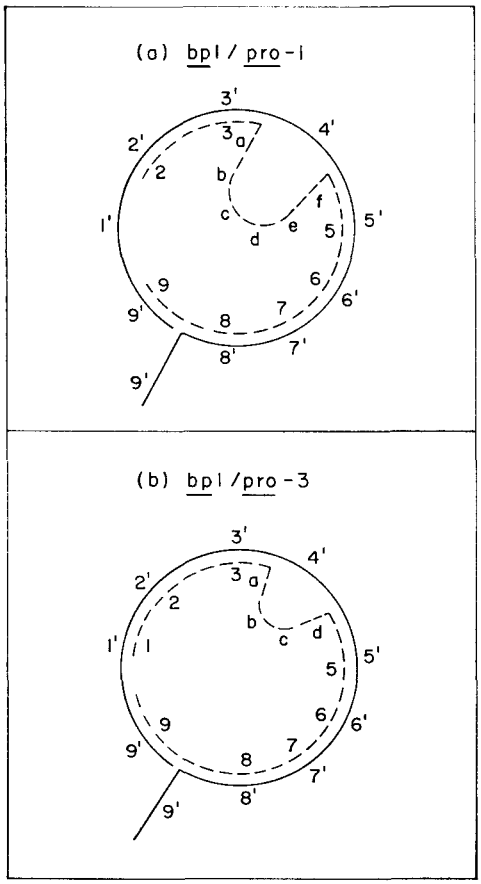

FIGURE 9.—A schematic diagram showing our interpretation of the DNA heteroduplexes between P22 *bp1 tet*^{R} [*att int*] ▽ and the proline phages. The solid line represents the *bp1* DNA strand and the dashed line represents the proline phage DNA.

the nonhomology region of a *bp1*/wild-type heteroduplex is 15%, representing the P22 DNA which is deleted in *bp1*, whereas the length of the *bp1* strand in the nonhomology region of the same heteroduplex is 10%, representing the remainder of the Tc-10 insertion left in *bp1*.

Knowing the size of the *pro-1* insertion (e.g., from Figure 8c), we can predict that the length of the *bp1* strand in the nonhomology region of a *bp1/pro-1* heteroduplex should still be 10%, representing the remainder of the Tc-10 insertion. The length was measured and found to be 12.3 ± 3.2% (Figure 8e). The length of the *pro-1* strand is expected to be 15% + 13% = 28%, representing the P22 DNA deleted from *bp1* (15%) and the proline genes (13%) added in P22*pro-1* for which there is no homology in *bp1*. The length of the *pro-1* strand as determined by measuring is 30.1 ± 6.1% (Figure 8e). Within the limits of error, there is agreement between predictions and the actual measurements.

We can make the same calculations for the *pro-3/bp1* heteroduplex. The length of the *bp1* strand in the nonhomology region of a *pro-3/bp1* heteroduplex should be 10%, representing the remainder of the Tc-10 insertion; the measured length for that strand is 9.7 ± 1.7% (Figure 8f). The length of the *pro-3* strand in the nonhomology region of a *pro-3/bp1* heteroduplex is expected to be 15% + 3% = 18%, representing the P22 DNA deleted from *bp1* (15%) and the proline genes (3%) added in P22*pro-3*; the measured length for that strand is 17.6 ± 3.1 (Figure 8f). Again, the agreement between predictions and the actual measurements is well within experimental error.

*The P22*pro-1 *and P22*pro-3 *substitutions are at the phage attachment site*: P22*pro-1* carries the *proA* and *proB* genes (JESSOP 1972) which are located to the left of the P22 prophage attachment site on the *Salmonella typhimurium* chromosome (SMITH and LEVINE 1965; SMITH and STOCKER 1966; ITIKAWA and DEMEREC 1968); thus, we could imagine that P22*pro-1* was formed in an abnormal excision event (Figure 10) as envisioned by CAMPBELL (1962). The hybrid attachment site formed by such an abnormal excision might account for

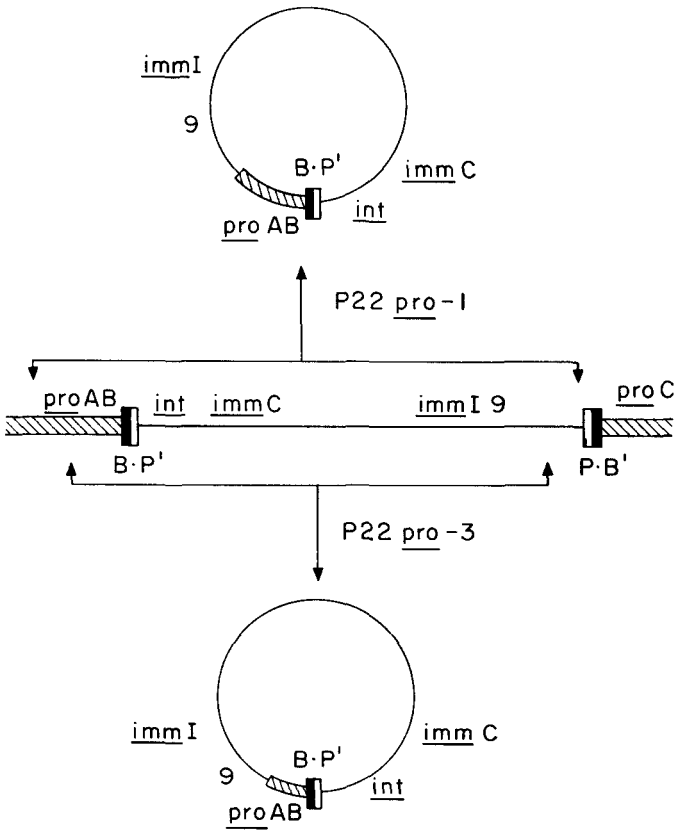

FIGURE 10.—A model for the formation of P22*pro-1* and P22*pro-3* by abnormal excision (CAMPBELL 1962) of the P22 prophage.

the failure of P22*pro-1* to integrate normally. The formation of P22*pro-3*, which also contains a substitution of the proline genes and fails to integrate normally, can be explained in the same way (Figure 10).

If P22*pro-1* and P22*pro-3* were formed by the mechanism outlined in Figure 10, the hybrid attachment site (B·P′), which marks the endpoint of the proline substitution, should be located at the same place in P22*pro-1* and P22*pro-3*. The distance between the Tc-10 insertion and the distal endpoint of the *pro-1* substitution [(5.8 ± 1.2)% + (0.4 ± 0.3)% = (6.2 ± 1.5)%] (see Figure 8a) is identical to the distance between the Tc-10 insertion and the distal endpoint of the *pro-3* substitution [(3.0 ± 1.4)% + (3.1 ± 0.8)% = (6.1 ± 2.2)%] (see Figure 8b), strongly supporting the idea that P22*pro-1* and P22*pro-3* were indeed formed by an abnormal excision as envisioned by CAMPBELL (1962) and that B·P′, the hybrid attachment site, is located at the distal endpoint of the proline substitution.

Since the 6% insertion of bacterial genes in P22*pro-3* carries *proAB*$^+$, the *proA* and *proB* genes must be located within 6% (the length of the wild-type P22 genome) of the attachment site, assuming that P22*pro-3* was formed by the single excision pictured in Figure 10.

Constructing a physical map of the region of the P22 genome near the prophage attachment site: In the previous section, we concluded that the distal endpoint (relative to the Tc-10 insertion) of the proline substitutions represented the site of B·P′, the hybrid attachment site (see Figure 10). Knowing that the Tc-10 insertion is located a distance of 6% (the length of a wild-type P22 genome) from the distal endpoint of the proline substitutions (see Figures 8a, b), and that the Tc-10 insertion is located on the gene *9* side of the attachment site (see Figure 7), we place the Tc-10 insertion on the gene *9* side of a point 6% from the attachment site (Figure 11).

Defining the position of the Tc-10 insertion allows us to estimate the extent of the deletions which remove part of the Tc-10 insertion as well as some phage DNA in P22*bp1* *tet*^{R} [*att int*]▽ and P22*bp5* *tet*^{S} [*att int*]▽ (CHAN *et al.* 1972). TYE, CHAN and BOTSTEIN (1974) found that P22*bp1* deleted 15% of wild-type P22 and retained a segment of the Tc-10 insertion equivalent to 10% of the wild-type P22 genome. Assuming that P22 *bp1* was formed by a single continuous deletion, we can locate the left endpoint of the *bp1* deletion so that a segment of the Tc-10 insertion equivalent to 10% of the wild-type P22 genome is retained. In order to account for the 15% deletion of P22 genes by the *bp1* deletion, the right endpoint of the *bp1* deletion must be located 9% to the right of the attachment site (Figure 11).

The genetic properties of P22*bp1* (CHAN *et al.* 1972; TYE, CHAN and BOTSTEIN 1974) are consistent with these physical endpoints:

1) P22*bp1* still carries the *tet*^{R} gene. SHARP, COHEN and DAVIDSON (1973) showed that the *tet*^{R} gene is located in the loop; this physical map leaves P22*bp1* with half of the loop.

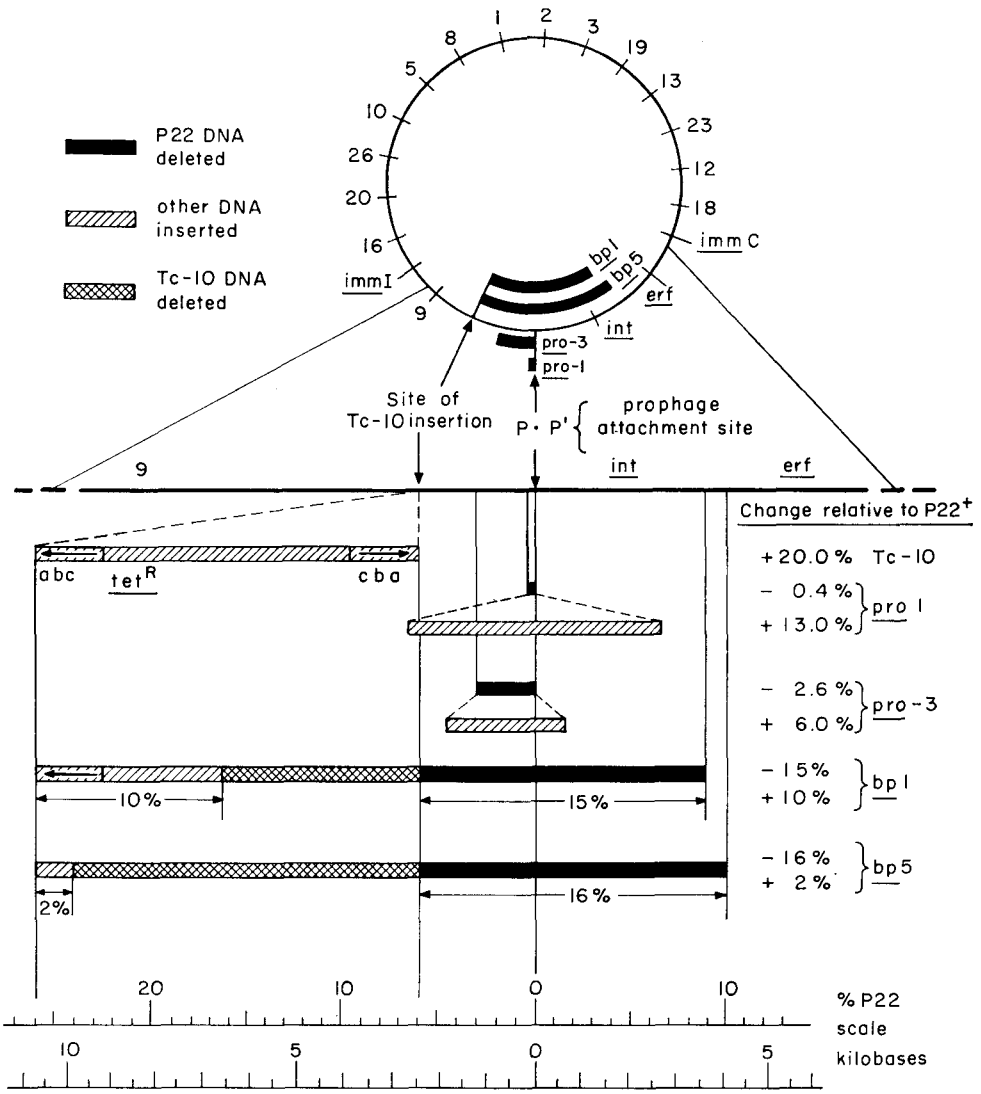

FIGURE 11.—A physical map of a portion of the P22 genome near the phage attachment site. The solid bars superimposed on the circular P22 genetic map represent portions of the P22 genome which are deleted in P22*bp1*, P22*bp5*, P22*pro-1* and P22*pro-3*. The site of the P22Tc-10 insertion is also indicated.

The region near the phage attachment site (P·P') is drawn in greater detail showing the insertions, deletions and substitutions. The sequence (a b c) represents the stem sequence (i.e., the inverted repeat) of the Tc-10 insertion. The scale at the bottom gives the dimensions as a percentage of the P22 wild-type homoduplex circumference or as kilobases.

The lengths are based on measurements from this paper and from TYE, CHAN and BOTSTEIN (1974).

2) P22*bp1* behaves as if it were *att*$^-$. This map shows that the *bp1* deletion has removed 6% of wild-type P22 DNA to the left of *att* and 9% of wild-type P22 DNA to the right of *att*.

3) P22*bp1* is *int*$^-$. Since the *int* gene is the closest known gene on the right side of *att*, this map suggests that the *int* gene must lie within 9% of the attachment site.

4) Since P22*bp1* is *erf*$^+$, the *erf* gene which is the closest gene to the right of *int* (BOTSTEIN and MATZ 1970) must be at least 9% to the right of the attachment site.

We can also estimate the extent of the deletion in P22*bp5*. P22*bp5* has deleted 16% of wild-type P22 and retained a segment of the Tc-10 insertion equivalent to 2% of the wild-type P22 genome (TYE, CHAN and BOTSTEIN 1974). The right endpoint of the *bp5* deletion must be close to the endpoint of the *bp1* deletion (Figure 11). However, the left endpoint of the *bp5* deletion must lie in the reverse duplication (in order to leave a segment of the Tc-10 insertion equivalent to 2% of the wild-type P22 genome behind). This physical map is also consistent with the genetic properties of P22*bp5* (CHAN *et al.* 1972; TYE, CHAN and BOTSTEIN 1974). Like P22*bp1*, P22*bp5* is *att*$^-$ and *int*$^-$. Since P22*bp5* has deleted the entire loop of the Tc-10 insertion, which presumably contains the *tet*^{R} genes, P22*bp5* should be *tet*^{S}, which it is.

The DNA contained in the 6% segment between the site of the Tc-10 insertion and the attachment site is dispensable for normal P22 growth since both P22*bp1* and P22*bp5* grow perfectly well, in spite of the fact that this region is completely deleted in both phages. Striking similarities were found in the genetic maps of the coliphage λ and the Salmonella phage P22 (BOTSTEIN, CHAN and WADDELL 1972); this nonessential region in the P22 genome between the tail gene (gene *9*) and the phage attachment site thus seems to be analogous to the λ *b2* region.

*The origin of P22*pro-1 *and P22*pro-3

All the evidence presented in this paper strongly suggests that P22*pro-1* and P22*pro-3* were formed by an abnormal excision of the P22 prophage as envisioned by CAMPBELL (1962). Especially compelling is the observation that the *pro-1* and *pro-3* substitutions share a common endpoint, the existence of which is explicitly predicted by the Campbell model.

The formation of P22*pro-1* and P22*pro-3* in Salmonella can be considered analogous to the formation of λ *gal* specialized transducing phages in *E. coli* since the *proAB* genes and the *gal* genes occupy similar positions with respect to the integrated prophage. Therefore, it is not surprising that P22*pro-1* and P22*pro-3* also share the *att*$^-$ phenotype characteristic of the λ *gal* phages (WEISBERG and GOTTESMAN 1969). This result implies that P22, like λ, requires an intact right-hand phage attachment site (P· in Figure 10) for efficient integration into the attachment site on the bacterial chromosome.

In our analysis of the heteroduplex structure of the *pro-1* substitution, we could not rule out the possibility that the *pro-1* substitution was actually a simple inser-

tion rather than an insertion-deletion. This alternate structure for the *pro-1* substitution is still compatible with the mechanism suggested above.

JESSOP (1972) reported that P22*pro-1* and P22*pro-3* were isolated from a stock of P22 which had been grown lytically using the agar plate method. However, our model for the origin of P22*pro-1* and P22*pro-3* necessarily assumes that the parental P22 phage was integrated prior to the abnormal excision event. Thus, it seems reasonable to assume that some of the phage must have integrated and excised during growth on the plate.

The origin of P22Tc-10

According to the Campbell model (CAMPBELL 1962), the Tc-10 insertion should be located next to the phage attachment site since the model assumes that the specialized transducing phage is generated next to the genes of interest (c.f., Figure 10). Instead, we find that the Tc-10 insertion is 6% of the length of a wild-type P22 genome away from the prophage attachment site (Figure 11). Furthermore, the Tc-10 insertion, as seen in heteroduplexes, has an unusual lariat-like structure which suggests that the insertion contains a nontandem reverse duplication. These observations suggest that the formation of P22Tc-10 is not consistent with the Campbell model.

Instead, we believe that P22Tc-10 was formed by the translocation of the intact tet^R element (including the inverted repetition) from the *R* factor chromosome to the P22 chromosome, since the structure of the Tc-10 insertion (TYE, CHAN and BOTSTEIN 1974) is identical to the structure of the tet^R element on the *R* factor (SHARP, COHEN and DAVIDSON 1973) from which P22Tc-10 was derived. More recent results (KLECKNER *et al.* 1975) suggest that the Tc-10 element can be excised from the P22 chromosome and inserted into different sites on the Salmonella chromosome.

How is the Tc-10 element translocated from one piece of DNA to another? We believe that the stem sequences (i.e. the sequences in the inverted repeat) are responsible for the integration and excision of the Tc-10 element since PTASHNE and COHEN (1975) have shown that the stem sequence of Tc-10 is identical to a known IS sequence—a piece of DNA which is known to insert into different sites on the bacterial chromosome (FIANDT, SZYBALSKI and MALAMY 1972; HIRSCH, STARLINGER and BRACHET 1972; MALAMY, FIANDT and SZYBALSKI 1972).

We would like to thank A. JESSOP for providing the P22 proline transducing phages and for sharing her unpublished results with us. We are grateful for the assistance of B.-K. TYE, E. V. LENK and J. A. KING in the use of the Biology Department Electron Microscope Facility. This research is supported by grants from N.I.H. (GM 18973) and the American Cancer Society (VC-18B). The computer facilities in the Research Laboratory of Electronics, M.I.T., were supported by NIH grant GM14940 to M. EDEN and I. T. YOUNG. One of us (D.B.) holds a Career Development Award from N.I.H. (GM70325). The other author (R.K.C.) was a trainee under a Microbiology Training Grant (GM-00602) to the Department of Biology, M.I.T., from the National Institute of General Medical Sciences.

The preparation of this manuscript was supported, in part, by N.I.H. grant GM17709 to L. H. HARTWELL and by a postdoctoral fellowship to R.K.C. by the Jane Coffin Childs Memorial Fund for Medical Research.

LITERATURE CITED

ADAMS, M. H., 1959 *Bacteriophages.* Wiley (Interscience), New York.

BEZDEK, M. and P. AMATI, 1968 Evidence for two immunity regulator systems in temperate bacteriophages P22 and L. Virology **36:** 701–703.

BOTSTEIN, D., 1968 Synthesis and maturation of phage P22 DNA. I. Identification of intermediates. J. Mol. Biol. **34:** 621–641.

BOTSTEIN, D. and M. J. MATZ, 1970 A recombination function essential to the growth of bacteriophage P22. J. Mol. Biol. **54:** 417–440.

BOTSTEIN, D., R. K. CHAN and C. H. WADDELL, 1972 Genetics of bacteriophage P22. II. Gene order and gene function. Virology **49:** 268–282.

CAMPBELL, A. M., 1962 Episomes. Advan. Genet. **11:** 101–145.

CHAN, R. K., 1974 Specialized transduction by bacteriophage P22. Ph.D. thesis. Massachusetts Institute of Technology, Cambridge, Mass.

CHAN, R. K. and D. BOTSTEIN, 1972 Genetics of bacteriophage P22. I. Isolation of prophage deletions which affect immunity to superinfection. Virology **49:** 257–267.

CHAN, R. K., D. BOTSTEIN, T. WATANABE and Y. OGATA, 1972 Specialized transduction of tetracycline resistance by phage P22 in *Salmonella typhimurium.* II. Properties of a high-frequency-transducing lysate. Virology **50:** 883–898.

DAVIS, R. W., M. SIMON and N. DAVIDSON, 1971 Electron microscope heteroduplex methods for mapping regions of base sequence homology in nucleic acids. pp. 413–428. In: *Methods in Enzymology,* Vol. XXI, part D. Edited by L. GROSSMAN and K. MOLDAVE. Academic Press, New York.

DUBNAU, E. and B. A. D. STOCKER, 1964 Genetics of plasmids in *Salmonella typhimurium.* Nature **204:** 1112–1113.

EBEL-TSIPIS, J. and D. BOTSTEIN, 1971 Superinfection exclusion by P22 prophage in lysogens of *Salmonella typhimurium.* I. Exclusion of generalized transducing particles. Virology **45:** 629–637.

FIANDT, M., W. SZYBALSKI and M. H. MALAMY, 1972 Polar mutations in *lac, gal,* and phage λ consist of a few IS-DNA sequences inserted with either orientation. Molec. Gen. Genetics **119:** 223–231.

GOTS, J. S., C. E. BENSON and S. R. SHUMAS, 1972 Genetic separation of hypoxanthine and guanine-xanthine phosphoribosyl transferase activities by deletion mutations in *Salmonella typhimurium.* J. Bacteriol. **112:** 910–916.

GOUGH, M., 1968 Second locus of bacteriophage P22 necessary for the maintenance of lysogeny. J. Virol. **2:** 992–998.

GOUGH, M. and M. LEVINE, 1968 The circularity of the phage P22 linkage map. Genetics **58:** 161–169.

HIRSCH, H.-J., P. STARLINGER and P. BRACHET, 1972 Two kinds of insertions in bacterial genes. Mol. Gen. Genet. **119:** 191–206.

HOPPE, I. and J. ROTH, 1974 Specialized transducing phages derived from Salmonella phage P22. Genetics **76:** 633–654.

ISRAEL, V., 1967 The production of inactive phage P22 particles following induction. Virology **33:** 317–322.

ISRAEL, J. V., T. F. ANDERSON and M. LEVINE, 1967 *In vitro* morphogenesis of phage P22 from heads and base-plate parts. Proc. Natl. Acad. Sci. U.S. **57:** 284–291.

ITIKAWA, H. and M. DEMEREC, 1968 *Salmonella typhimurium* proline mutants. J. Bacteriol. **95:** 1189–1190.

JESSOP, A. P., 1972 A specialised transducing phage of P22 for which the ability to form plaques is associated with transduction of the *pro*AB region. Molec. Gen. Genetics **114:** 214–222. ——, 1976 Specialized transducing phages derived from phage P22 that carry the *proAB* region of the host, *Salmonella typhimurium*: genetic evidence for their structure and mode of transduction. Genetics **83:** 459–475.

KAYE, R., J. BARRAVECCHIO and J. ROTH, 1974 Isolation of P22 specialized transducing phage following F′-episome fusion. Genetics **76:** 655–667.

KELLENBERGER, G., M. L. ZICHICHI and J. WEIGLE, 1961 A mutation affecting the DNA content of bacteriophage lambda and its lysogenizing properties. J. Mol. Biol. **3:** 399–408.

KLECKNER, N., R. K. CHAN, B.-K. TYE and D. BOTSTEIN, 1975 Mutagenesis by insertion of a drug-resistance element carrying an inverted repetition. J. Mol. Biol. **97:** 561–575.

LEVINE, M., 1957 Mutations in the temperate phage P22 and lysogeny in Salmonella. Virology **3:** 22–41. ——, 1972 Replication and lysogeny with phage P22 in *Salmonella typhimurium*. Curr. Top. Microbiol. Immunol. **58:** 135–156.

LEVINE, M. and R. CURTISS, 1961 Genetic fine structure of the C region and the linkage map of phage P22. Genetics **46:** 1573–1580.

MALAMY, M. H., M. FIANDT and W. SZYBALSKI, 1972 Electron microscopy of polar insertions in the *lac* operon of *Escherichia coli*. Molec. Gen. Genetics **119:** 207–222.

MIYAKE, T. and M. DEMEREC, 1960 Proline mutants of *Salmonella typhimurium*. Genetics **45:** 755–762.

PTASHNE, K. and S. N. COHEN, 1975 Occurrence of insertion sequence (IS) regions on plasmid deoxyribonucleic acid as direct and inverted nucleotide sequence duplications. J. Bacteriol. **122:** 776–781.

RHOADES, M., L. A. MACHATTIE and C. A. THOMAS, JR., 1968 The P22 bacteriophage DNA molecule. I. The mature form. J. Mol. Biol. **37:** 21–40.

SHARP, P. A., S. N. COHEN and N. DAVIDSON, 1973 Electron microscope heteroduplex studies of sequence relations among plasmids of *Escherichia coli*. II. Structure of drug resistance (R) factors and F factors. J. Mol. Biol. **75:** 235–255.

SMITH, H. O., 1968 Defective phage formation by lysogens of integration deficient phage P22 mutants. Virology **34:** 203–223.

SMITH, H. O. and M. LEVINE, 1964 Two sequential repressions of DNA synthesis in the establishment of lysogeny by phage P22 and its mutants. Proc. Natl. Acad. Sci. U.S. **52:** 356–363. ——, 1965 Gene order in prophage P22. Virology **27:** 229–231. ——, 1967 A phage P22 gene controlling integration of prophage. Virology **31:** 207–216.

SMITH, S. M. and B. A. D. STOCKER, 1966 Mapping of prophage P22 in *Salmonella typhimurium*. Virology **28:** 413–419.

SMITH-KEARY, P. F., 1966 Restricted transduction by bacteriophage P22 in *Salmonella typhimurium*. Genet. Res. **8:** 73–82.

STREISINGER, G., J. EMRICH and M. M. STAHL, 1967 Chromosome structure in phage T4. III. Terminal redundancy and length determination. Proc. Natl. Acad. Sci. U.S. **57:** 292–295.

SUSSKIND, M. M., A. WRIGHT and D. BOTSTEIN, 1971 Superinfection exclusion by P22 prophage in lysogens of *Salmonella typhimurium*. II. Genetic evidence for two exclusion systems. Virology **45:** 638–652.

TYE, B.-K., R. K. CHAN and D. BOTSTEIN, 1974 Packaging of an oversize transducing genome by *Salmonella* phage P22. J. Mol. Biol. **85:** 485–500.

TYE, B.-K., J. A. HUBERMAN and D. BOTSTEIN, 1974 Nonrandom circular permutation of phage P22 DNA. J. Mol. Biol. **85:** 501–532.

WATANABE, T., Y. OGATA, R. K. CHAN and D. BOTSTEIN, 1972 Specialized transduction of tetracycline resistance by phage P22 in *Salmonella typhimurium*. I. Transduction of R factor 222 by phage P22. Virology **50**: 874–882.

WEISBERG, R. A. and M. E. GOTTESMAN, 1969 The integration and excision defect of bacteriophage λ *dg*. J. Mol. Biol. **46**: 565–580.

WING, J. P., 1968 Transduction by phage P22 in a recombination-deficient mutant of *Salmonella typhimurium*. Virology **36**: 271–276.

Corresponding editor: H. ECHOLS